Double-reconnected magnetic structures driven by Kelvin-Helmholtz vortices at the Earth's magnetosphere

D. Borgogno, F. Califano, M. Faganello, and F. Pegoraro

Citation: Physics of Plasmas (1994-present) **22**, 032301 (2015); doi: 10.1063/1.4913578
View online: http://dx.doi.org/10.1063/1.4913578
View Table of Contents: http://scitation.aip.org/content/aip/journal/pop/22/3?ver=pdfcov
Published by the AIP Publishing

Double-reconnected magnetic structures driven by Kelvin-Helmholtz vortices at the Earth's magnetosphere

D. Borgogno,[1] F. Califano,[1] M. Faganello,[2] and F. Pegoraro[1]
[1]*Physics Department, University of Pisa, 56127 Pisa, Italy*
[2]*Aix-Marseille University, CNRS, PIIM UMR 7345, 13397 Marseille, France*

(Received 10 December 2014; accepted 12 February 2015; published online 2 March 2015)

In an almost collisionless magnetohydrodynamic plasma in a relatively strong magnetic field, stresses can be conveyed far from the region where they are exerted, e.g., through the propagation of Alfvèn waves. The forced dynamics of line-tied magnetic structures in solar and stellar coronae (see, e.g., A. F. Rappazzo and E. N. Parker, Astrophys. J. **773**, L2 (2013) and references therein) is a paradigmatic case. Here, we investigate how this action at a distance develops from the equatorial region of the Kelvin-Helmholtz unstable flanks of the Earth's magnetosphere leading to the onset, at mid latitude in both hemispheres, of correlated double magnetic field line reconnection events that can allow the solar wind plasma to enter the Earth's magnetosphere. © *2015 AIP Publishing LLC*.
[http://dx.doi.org/10.1063/1.4913578]

I. INTRODUCTION

The interaction between the solar wind (SW) and the Earth's magnetosphere (MS) displays in full the wide variety of phenomena that enrich the nonlinear dynamics of magnetized streaming plasmas. It also affects the conditions of near Earth space through the magnetic perturbations that characterize the time variability of what we call now "space weather." In the present paper, we are interested in the mechanisms through which this interaction leads to the penetration of SW plasma into the MS.

It is widely accepted that magnetic field line reconnection controls the transport properties of the SW plasma into the Earth's MS at low latitudes when the SW magnetic field is mostly southward. In these conditions, the geomagnetic field lines are anti-parallel to those of the SW, leading to the typical configuration for which magnetic reconnection is expected to occur[1] and has actually been observed.[2] On the contrary during northward conditions, magnetic reconnection is suppressed and the system should reach a relatively quiet situation. This is not what is observed, since also in this case, satellite observations show the entry of ion populations denser and colder than the local plasma[2] in the near-Earth plasma sheet flanks. These observations suggest an enhancement of plasma transport and therefore the need to find the driver responsible for the observed dynamics leading to plasma mixing at the interface between the MS and the SW. The Kelvin-Helmholtz instability (KHI) on the flanks of the MS is considered as one of the mechanisms for populating the low latitude boundary layer[1,3–5] during periods of northward interplanetary magnetic field. The KHI can grow in the low latitude boundary layer because of the persistent velocity shear between the SW plasma flow and the MS plasma at rest. Furthermore, in this region, the magnetic field is almost perpendicular to the equatorial plane so that the low magnetic tension is not able to suppress the development of the instability.

Several articles in the literature have reported numerical investigations of the KHI at the interface between the MS and the SW with the aim of understanding the induced transport across the magnetopause in the equatorial plane, assuming a simple two-dimensional (2D) geometry. In this case, the magnetic field direction is mainly perpendicular to the shear flow direction, and spatial variations along the magnetic field are neglected. This analysis made it possible to investigate vortex induced reconnection (VIR),[6] the vortex pairing process in magnetized plasma,[7,8] and to identify several different types of secondary instabilities taking place on the shoulder of the vortex chain emerging from the development of the KHI (see Ref. 9 and references therein). These secondary instabilities have been shown to occur and compete in their nonlinear development depending on the structure of the initial large-scale fields (in particular, the velocity, density and magnetic field) and enhance the transport properties of the KH vortices.[8,10,11] Of particular relevance is the role of the magnetic reconnection instability which develops when a weak in-plane magnetic field component is present. In this case, KH vortices are responsible for the stretching and amplification of the in-plane magnetic field lines, leading to the formation of intense current layer that is unstable to magnetic reconnection. Numerical simulations performed both in fluid and in fully-kinetic regimes have shown that magnetic coherent structures, i.e., magnetic islands, develop inside or between the KH vortices[5,12–14] and are able to cross the MS boundary.[14,15] The presence of magnetic islands between flow vortices at the magnetopause has been recently detected by THEMIS mission observations,[16] showing a qualitative agreement with the numerical predictions. These 2D simulations have been extended to 3D kinetic simulations that, while spatially limited to the low latitude region, were able to show the formation of oblique *magnetic flux ropes*.[17]

There are various reasons why the 2D approximation is a questionable assumption. It is well known for instance that the concept of magnetic islands breaks down in 3D systems. Numerical simulations of tearing mode instabilities in a static Harris-type current layer for collisionless plasmas have

shown the formation in the reconnection regions of highly turbulent states due to the interaction between magnetic flux ropes[18] or the stochastic behavior of the magnetic field lines.[19] An even more fundamental reason why a fully 3D approach is needed in order to treat the interaction between the SW and the Earth's MS properly arises from the complex topology of the magnetic field at the MS flank. Here, magnetic field lines connecting Earth to Earth and Earth to open space and open space to open space can coexist. This leads to a complex pattern of field lines that cross (in some cases more than once) and/or link plasma regions that are either tied to Earth or are advected by the SW. Since, aside for local disconnections and reconnections, these magnetic connections are essentially preserved by the plasma evolution, the plasma dynamics in such a structured magnetized system is dominated by *non-local* effects. In the MS configuration, we can view the magnetic field lines as some sort of flexible "rods" that allow for a very effective momentum and energy transfer between plasma regions at different latitudes[20,21] on Alfvèn times. This non-local effect is even more significant when we include, by modelling the width of the shear flow layer between the MS and the SW in such a way that it widens far from the equatorial region, the fact the strength of the KHI is largest in the equatorial region and decreases with latitude. Thus, magnetic reconnection and the KHI need not occur in the same (low latitude) region. This effect of the high-latitude stabilization of the KHI modes and the magnetic action at a distance cannot be accounted for by 3D simulations limited to the equatorial region which can however investigate the role of kinetic effects.[17] On the other hand, kinetic effects cannot yet be addressed on a global spatial scale with present computational resources.

In Refs. 21 and 20, 3D fluid plasma simulations of the onset and development of the magnetic reconnection associated with the KH vortices that include the effect of the global magnetic topology and differential advection have been performed by devising a simplified 3D description of the MS flanks, which retains the high-latitude stabilization of the KHI. In this case, the vortices in the equatorial region, where the conditions for KHI are more favourable, drive a completely different plasma dynamics if compared to 2D configurations or in general to configurations limited to the equatorial region. In this 3D configuration, the KH vortices act as a forcing at a distance driver and influence the magnetic field dynamics far away from the equatorial region. This leads to the formation of extended current sheets at mid latitude where reconnection occurs. Moreover, due to the stretching caused by the differential advection, the same MS and SW field lines that cross a current sheet in the northern hemisphere, cross also a current sheet in the southern one. Thus once these lines have reconnected in one hemisphere, they could reconnect a second time, again at mid-latitude but in the opposite hemisphere. Actually, this evolution is forced to occur by topological constraints. Indeed, once the first reconnection process has occurred, the resulting lines become braided and a second reconnection process must occur in order to unbraid field lines and relax their magnetic tension.[20] As a result, magnetic field lines are formed, which are embedded at high latitudes into the MS plasma in both hemispheres but cross the SW plasma at low latitudes. By generating such lines, mid latitude double reconnection provides an effective transport channels for the entry of SW plasma into the Earth's MS. An observational validation of this mechanism has been recently presented in Ref. 25.

In the present paper, we analyze the vortex induced reconnection problem in a plasma fluid description retaining the high latitude stabilization of KHI, as in Refs. 20 and 21, but adopting a new equilibrium configuration that although still idealized, provides a better representation of the actual geometry of the magnetic configuration in the region around the Earth's MS, including the curvature of the MS lines at the dawn-dusk terminator. We investigate the spatial structure of the mid latitude current sheets, that naturally develop during the KHI evolution, which are found to exhibit quasi-2D features. We show that magnetic reconnection is responsible for the break-up of magnetic field lines at mid latitude in both hemispheres and that most field lines that that have been once reconnected in one hemisphere readily experience a second reconnection in the other hemisphere. This leads to a rather complex 3D magnetic structure, where 2D features, such as the plasmoid instability[22–24] of thin current sheets, combine with purely 3D effects that arise from the cross talking between current layers in different hemispheres and from the turning and twisting due to the KH vortices in the equatorial region. The reconnected magnetic structures in the northern and in the southern hemispheres are linked by highly twisted magnetic flux tubes whose cross section increases with time and that consist of field lines that are part of the MS at high latitudes but are embedded in the SW in the low-latitude equatorial region. These tubes represent the channel by which SW particles can flow towards the Earth in this mid latitude double reconnection scenario.[20,21]

II. PLASMA MODEL AND GEOMETRICAL CONFIGURATION

We analyze the plasma behavior at the Earth magnetopause by using the resistive Hall magnetohydrodynamic model (R-H-MHD) that can be viewed as a two-fluid description of a plasma when electron inertia is neglected. Resistivity is introduced in order to allow within a fluid description for a controlled development of magnetic reconnection that, in the low collisionality environment under consideration, would instead occur because of electron phase space effects. Choosing the ion skin depth d_i, the ion cyclotron frequency Ω_{ci} and the ion mass m_i as units, the R-H-MHD equations supplemented by the adiabatic closure in Eq. (3) read

$$\frac{\partial n}{\partial t} + \nabla \cdot (n\mathbf{U}) = 0, \tag{1}$$

$$\frac{\partial n\mathbf{U}}{\partial t} + \nabla \cdot \left[(n\mathbf{UU}) + \left(P\bar{\bar{I}} - \mathbf{BB} \right) \right] = 0, \tag{2}$$

$$\frac{\partial nS}{\partial t} + \nabla \cdot (nS\mathbf{U}) = 0, \qquad \text{with} \qquad S = P_{therm} n^{-5/3}, \tag{3}$$

$$\frac{\partial \mathbf{B}}{\partial t} - \nabla \times \left(-\mathbf{U} \times \mathbf{B} + \frac{\mathbf{J}}{n} \times \mathbf{B} + \eta \mathbf{J} \right) = 0, \tag{4}$$

where n is the plasma particle density, $\mathbf{U}$ is the fluid velocity, $\mathbf{B}$ is the magnetic field, $P = P_i + P_e + B^2/2 = P_{therm} + B^2/2$ is the sum of the thermal and the magnetic pressure, $\mathbf{J} = \nabla \times \mathbf{B}$ is the current density, η is the plasma resistivity, and nS is the entropy density. This model provides the simplest description suitable for describing the low collisionality, $\beta \sim 1$ plasma typically observed at the flank magnetopause.

These equations are integrated numerically in a 3D Cartesian configuration with the direction perpendicular to the magnetopause, at the equatorial plane, along the x-axis, the northward direction along the z-axis and the y-direction aligned along the SW flow. Open transparent boundary conditions are assumed along the x-axis,[15] while periodicity is used in the (y, z) plane. The numerical solver is based on a standard third order Adam-Bashforth method for temporal discretization and uses a sixth-order explicit scheme for spatial derivative along the y,z-directions and sixth-order compact finite difference scheme with spectral-like resolution for spatial derivative along the x-direction.[26] Numerical noise is controlled by adopting explicit sixth-order filters along the periodic y,z-directions and a sixth-order spectral-like filtering scheme along the x-direction.[26]

In order to model the MS flanks, we adopted an ideal magnetohydrodynamic equilibrium configuration, varying in the (x, z)-plane and constant along y, which reproduces the high-latitude stabilization of the KH instability and the dipolar curvature of MS lines near the dawn-dusk terminator. The magnetic field is described by a flux function related to the component of the vector potential along the ignorable y-direction.[27] In the case under consideration, the flux function corresponds to the y-component of the vector potential $A_{eq,y}$, with[21]

$$A_{eq,y}(x,z) = \frac{4}{5}(x - L_x) + \frac{L_z}{10\pi}\sinh\left(2\pi\frac{x - L_x}{L_z}\right)\cos\left(2\pi\frac{z}{L_z}\right), \tag{5}$$

where L_x and L_z are the numerical box lengths along x and z, respectively, $-L_z/2 < z < L_z/2$, $0 < x < L_x$. All other equilibrium quantities are functions of this vector potential component and are thus constant along the projections of magnetic field lines in the 2D (x, z) plane. This configuration makes the gradients along the magnetic field lines vanish, as consistent with the collisionless plasma behavior, where the parallel diffusion would rapidly suppress such gradients. The y-component of the equilibrium velocity is given by

$$U_{eq,y}(x,z) = \frac{1}{2}\tanh\left[\frac{A_{eq,y}(x,z) - L_{GS}}{L_{eq}}\right], \tag{6}$$

corresponding to a shear layer with half width $L_{eq} = 12/5 + 3/5\cosh[(2\pi/3)(L_x/L_z)]$ (chosen as three times the equilibrium scale $\partial A_{eq,y}/\partial x|_{z=0,\,x=2L_x/3}$) and whose position depends on $L_{GS} = -(4/15)L_x - (L_z/10\pi)\sinh[(2\pi/3)(L_x/L_z)] \equiv A_{eq,y}(z = 0, x = 2L_x/3)$.

Equilibrium density and entropy are taken to be homogeneous in order to inhibit a rapid development of other secondary instabilities[10,14,29] and to focus on magnetic reconnection. Furthermore, we consider a subsonic regime, which is the typical one adopted for the study of the low latitude boundary layer problem. Indeed taking $n = S = 1$ at $t = 0$, the sonic and alfvénic Mach numbers read $M_s = 0.77$ and $M_A = 1$, where the Alfvén velocity V_A is evaluated at $x = L_x$, $z = 0$. For later convenience, we introduce a passive tracer with initial distribution given by $Tr_{eq}(x, z) = 0.6 + 0.8\ U_{eq,y}(x, z)$ that is advected by the fluid velocity.

For the size of the computational box, we adopt $L_x = 90$, $L_y = 30\pi$, and $L_z = 360$. The 2D equilibrium configuration is shown in Fig. 1, where the isocontours of the magnetic flux function $A_{eq,y}$ (white solid lines) are overplotted on the shaded isocontour (from blue to red) of $U_{eq,y}$. The white dashed line, where $U_{eq,y} = 0$, represents the boundary between the MS (blue) and the SW (red) plasma regions. The fact that the plasma velocity is not null inside the MS is due to the fact that in our description, we use a reference frame moving with half the SW speed. The equilibrium configuration given by Eq. (5) is a modification of the "hourglass-like" configuration adopted in Ref. 21 and is constructed so as to mimic more accurately the actual geometry of the magnetic field into the region around the magnetopause. In particular, the magnetic field does not exhibit any symmetry across the boundary between the MS and the SW plasma, contrary to Ref. 21, where the magnetic field at the border between the two plasmas is completely directed along z. In fact, in the equilibrium (5), the magnetic surfaces become flatter as the distance from Earth increases, as consistent to the fact that the interplanetary magnetic field line tends to be locally straight.

The z-dependence of the equilibrium configuration makes the velocity shear stronger at the equatorial plane than at higher latitudes. As a consequence, according to the

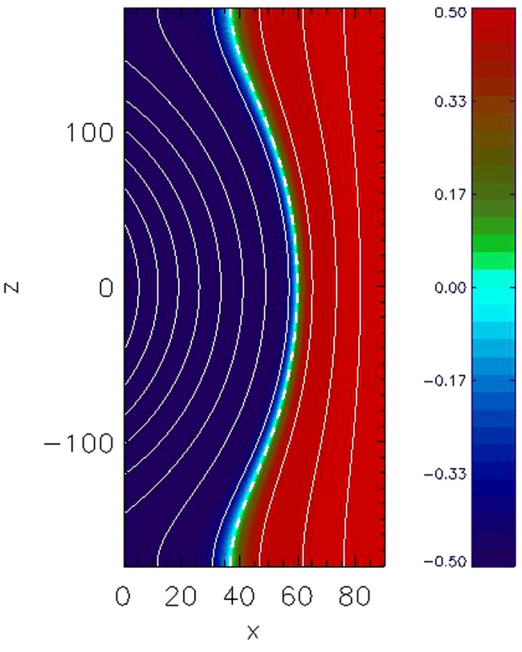

FIG. 1. Isocontour of the magnetic flux function $A_{eq,y}(x, z)$ (white solid lines) and colour isocontour (from blue to red) of the equilibrium velocity $U_{eq,y}(x, z)$. The white dashed line, where $U_{eq,y} = 0$, corresponds to the boundary which separates the MS (on the left) and the SW plasma (on the right).

simplified 2D description where the linear growth rate of the KHI is proportional to the equilibrium velocity gradient in the plane,[8] we expect the instability to develop earlier at low latitudes. In this way, we can mimic the high-latitude stabilization of the KHI. In the 3D Earth's MS configuration, this stabilization arises from the fact that the plasma kinetic energy dominates at low latitudes where the magnetic field is mainly perpendicular to the equatorial plane whereas the magnetic energy dominates at the higher latitudes, where the magnetic tension of the magnetic field component parallel to the flow prevents the vortex formation.

For the parameters that we have chosen, the $m_y = 2$ mode corresponds to the fast growing mode (FGM) at the equator, where m_y is the mode number of the KHI along the periodic y-direction. The adopted parameters are representative of the typical values of the physical quantities that can be observed at the outer MS. In particular, they are related to the dynamics of vortices with typical size much greater than the ion skin depth d_i. The KHI is thus able to generate two large-scale ($\lambda_{FGM} \approx 50 d_i$) vortices at the equator. Fig. 2 shows the passive tracer field in the (x, y) plane at $t = 700$, i.e., before the onset of the magnetic reconnection instability, at four different latitudes in the southern hemisphere: no vortices develop at the highest latitudes ($z = -180$ d_i and $z = -120$ d_i sections), while rolled-up vortices occur in the equatorial region. In this early phase, the KH vortices exhibit a north-south symmetry across the equatorial plane.

III. MID LATITUDE CURRENT LAYERS AND MAGNETIC FIELD LINE RECONNECTION

In Refs. 20 and 21, it has been shown that in 3D configurations that model the high-latitude stabilization of the KHI, the differential advection of the magnetic field lines frozen into the fluid velocity field at different latitudes creates strong current sheets where magnetic reconnection will eventually occur. In fact magnetic field lines, embedded at low latitudes in the growing KH vortices that have no net velocity along y, are advected in opposite directions at high latitudes by the unperturbed plasma flows. As a consequence, the MS and interplanetary magnetic field lines get bent and arched in opposite directions and extended current sheets are formed at mid latitude, in the northern and in the southern hemispheres. This dynamics occurs also in our new simulations, as shown in Fig. 6, left frame, where we can observe a MS (blue) magnetic field line and an interplanetary (red) one, which cross the northern and southern current sheets (pale blue isocontour surfaces of the magnitude of the current density) with different orientations.

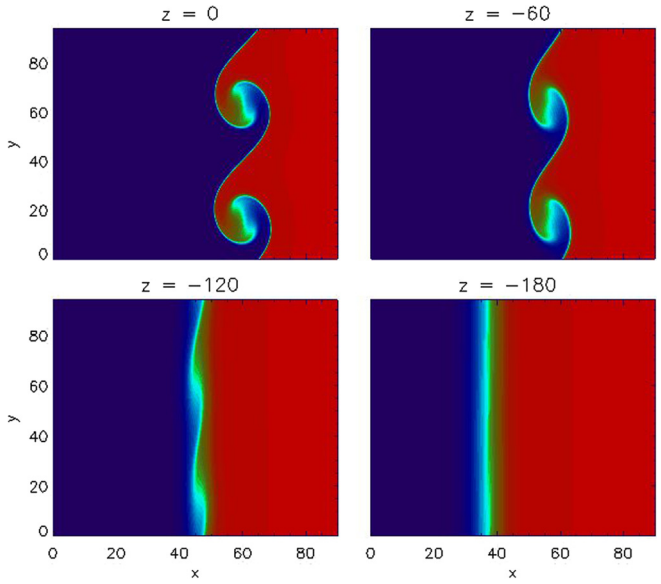

FIG. 2. Decrease with latitude of the KH vortices in the southern hemisphere. The shaded isocontour of the passive tracer field is shown at the $z = 0$, $z = -60d_i$, $z = -120d_i$, and $z = -180d_i$.

The scope of the new simulations discussed in the present article is twofold. First, we aim to investigate the spatial structure and nonlinear dynamics of these mid latitude current layers so as to document the development of magnetic reconnection, in a configuration that retains the magnetopause curvature. Second, we follow field lines that cross these current layers and that have been reconnected at least once in order to see how rapidly and with which "probability" they get reconnected twice so as to quantify the effectiveness of the double mid latitude reconnection in allowing the SW plasma to penetrate the MS plasma. In addition, we find that the combination of the forcing due to the KH vortices of the differential advection between the SW and the MS plasma and the magnetic cross talking between field lines reconnected in the northern and in the southern hemisphere leads to the formation of highly stretched and deformed magnetic structures as compared to the standard magnetic islands that are produced in 2D reconnection.

A. Internal structure of the current layers

Focusing first on the internal structure of the mid latitude current layer regions, we find that these layers take the form of thin sheets, with the periodicity of the KH vortices along y, and are highly elongated in the z direction with characteristic length $L_{cs_z} \approx 50\, d_i$. This high elongation makes the plasma behavior inside the current layers weakly dependent on the z coordinate and thus these layers might be expected to be reasonably well described by referring to an approximate 2D configuration in the presence of a relatively strong guide field with island-type structures and X- and O-points. In order to visualize their structure in the 3D setting of the simulations, we took a mid plane section (perpendicular to the z-direction) at the position of the current maximum inside a layer and developed a procedure based on the identification of the current sheet major axis in this section and its corresponding perpendicular direction. These axes define a Cartesian frame with origin at the current maximum aligned with the instantaneous orientation of the current sheet.

An example of the early current sheet structure in the southern mid latitude section is shown in Fig. 3, top frame, together with the set of cartesian axes ζ and ξ that we adopted for its representation. The current inside the layer, whose width is $\Delta \sim 10\, d_i$, is almost uniform along the layer, i.e., along ξ, and is dominated by the J_z component Fig. 3, lower left frame. On the contrary, the current gradient across the sheet, i.e., along ζ, is very sharp, leading to a layer

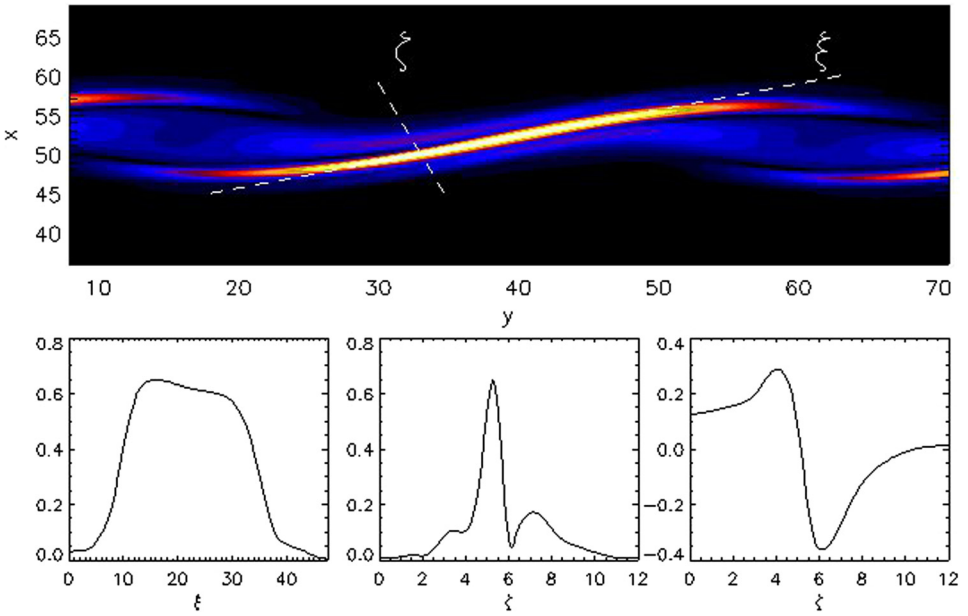

FIG. 3. Top frame: Isocontour of the total current distribution on the southern current sheet section at mid latitude. The ζ and ξ axes identify the reference frame adopted for the current sheet analysis. Bottom frame from left to right: total current profile versus ξ and versus ζ, the magnetic field component B_ξ versus ζ.

thickness of order $\delta \sim d_i$ Fig. 3, lower center frame. The magnetic field inside the layer has a dominant and uniform guide field component along z, while the in-plane magnetic field is almost completely aligned with the major axis of the current layer, reverses its sign across the $\zeta = const$ section where the current sheet reaches its maximum value (Fig. 3, lower right frame) and depends only weakly on ξ coordinate along the current sheet. In this mid plane section, the magnetic configuration reproduces almost exactly the standard sheared and symmetric magnetic field equilibrium adopted for the analysis of the 2D magnetic reconnection instability.

Looking now at the time evolution of the current inside the mid latitude layers, we find an early exponential growth for $t \lesssim 720$, as shown in Fig. 4, left frame, where the maximum value of the total current at the southern mid latitude section is plotted versus time. The growth rate $\gamma_{cs} = 0.03$ is comparable with the vortex rotation frequency at the equator $\omega = 0.04$, showing the ongoing nonlocal interplay between the low latitude dynamics of the KHI that continuously stretches the magnetic field lines and thus feeds the current layer at mid latitude, and the development of magnetic reconnection.

The exponential growth of the current sheet magnitude is followed by a saturation phase due to the competition between the magnetic flux convection into the sheet and its dissipation by reconnection. In order to follow this evolution in Fig. 4, right frame, we plot the maximum value versus time of $B \cdot \nabla Tr/|\nabla Tr|$, i.e., of the magnetic field component aligned with the gradient of the tracer Tr, along the major axis of the current layer. This quantity provides a reliable measure for the reconnection rate in a complex 3D framework by acting as a proxy for the magnetic field component normal to the reconnection layer in a 2D configuration. Since we initialized the simulation assuming Tr to be constant on the magnetic surfaces defined by the flux function $A_{eq,y}$, i.e., along field lines, finite values of $B \cdot \nabla Tr/|\nabla Tr|$ occur only where the MHD frozen-in law condition is violated. We find in Fig. 4 right frame that in the saturation phase, the maximum value of $B \cdot \nabla Tr/|\nabla Tr|$ has a quadratic dependence on time, as consistent with the growth of the reconnection instability in the so-called Rutherford regime.[28]

In Fig. 5, the shaded isocontours of $B \cdot \nabla Tr/|\nabla Tr|$ on the southern mid latitude section are shown at $t = 780$. An O-point (at (52.2, 39.8)) and two X-points (at (50.1, 32.3) and (54.3, 47.3)) can be identified and $B \cdot \nabla Tr/|\nabla Tr|$ is shown to be odd with respect to the O-point along the major axis of the current layer, as expected for a quantity that acts as proxy of the magnetic field component normal to the

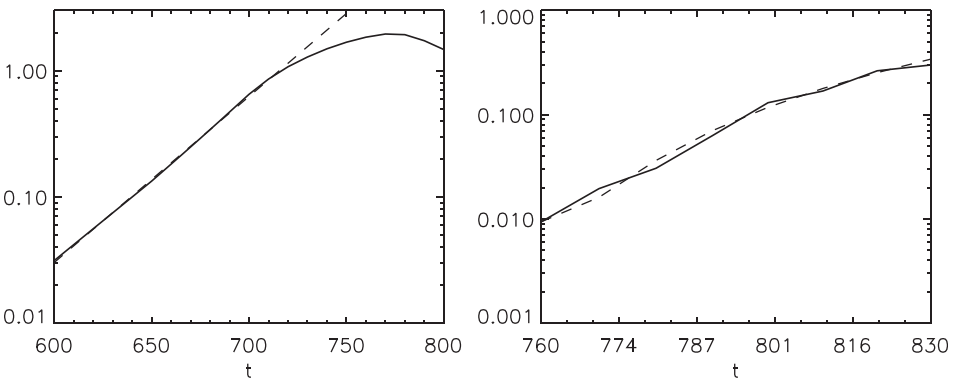

FIG. 4. Left frame: logarithmic plot of the maximum value of the total current at mid latitude versus time. The dashed line shows the exponential fit. Right frame: logarithmic plot of the maximum value of $B \cdot \nabla Tr/|\nabla Tr|$ versus time in the nonlinear saturation phase. The dashed line corresponds to the quadratic fit.

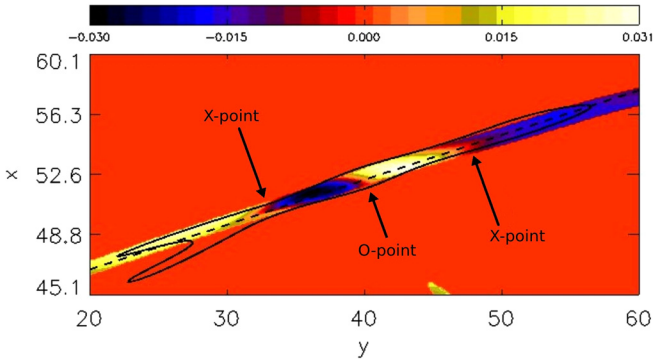

FIG. 5. Contour plot of $B \cdot \nabla Tr/|\nabla Tr|$ on the southern mid latitude section at $t = 780$. The black solid line identifies the boundary of the current sheet and the dashed line identifies its in-plane major axis. Note that $B \cdot \nabla Tr/|\nabla Tr|$ is odd along its major axis.

reconnection layer. At later times $t = 800$ (not shown here), the current layer becomes unstable to the onset of a plasmoid instability.[22–24]

B. Single versus double mid latitude reconnection

In order to see how field lines that have reconnected once in one hemisphere get reconnected a second time in the opposite hemisphere, we have taken a sample of field lines that cross the current layer in the northern hemisphere and followed them as they pass through the equatorial region and move into the southern hemisphere. A 3D picture that provides a general overview by stacking five x-y sections (high latitude north, mid latitude north, equatorial region, mid latitude south, high latitude south) and by following the field lines going through a current layer at mid latitude north, through the KH vortices in the equatorial region and finally crossing into the southern hemisphere, is shown in Fig. 6, right frame. In particular, we see that the yellow and green lines, that are connected, in the high latitude north section, to the MS and SW plasma, respectively, change their connectivity in the northern current sheet and cross the SW and MS plasma, respectively, in the equatorial region and in the high latitude south section. These lines originate from pristine magnetospheric and interplanetary lines (as blue and red lines in the left frame) that have experienced reconnection in the northern current sheet. Yellow and green lines still cross the southern current sheet with different orientations where eventually reconnection can occur generating double reconnected lines, as the violet and black lines plotted in the right frame.

A clearer and more quantitative description of this process is obtained by looking at the behavior of a set of magnetic field lines. Specifically, we want to see whether or not, at which latitude, and how many times, a given field line leaves the blue (MS) or the red (SW) tracer region and cross into the red or into the blue region, respectively. Note that each crossing corresponds to a reconnection event that has made the field line jump from the MS plasma to the SW plasma or viceversa.

This analysis has been carried out by solving numerically the magnetic field line equations $d\mathbf{x}/d\tau = \mathbf{B}(\mathbf{x})$, where $\mathbf{x}(\tau)$ is a field line path in the $3D$ space and τ is any convenient parameter playing the role of "field line time." The magnetic field $\mathbf{B}$

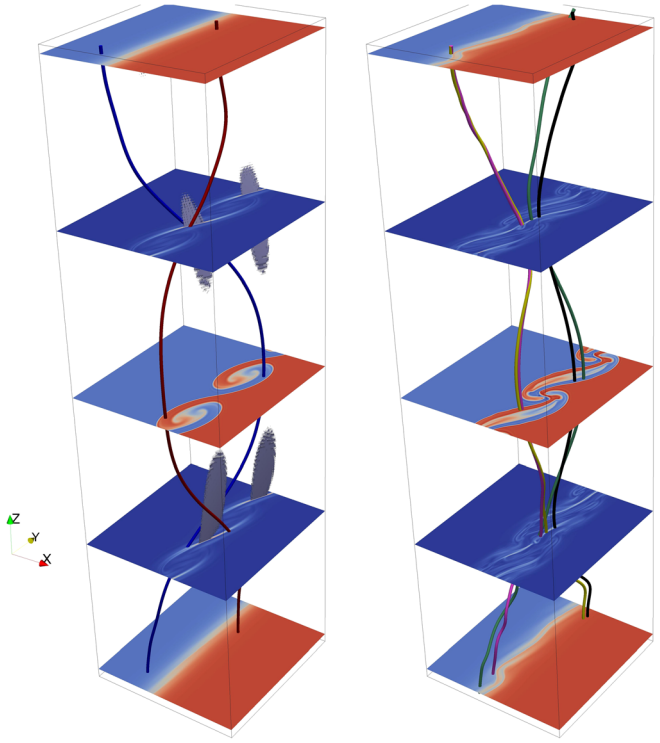

FIG. 6. Global overview obtained by stacking three x-y sections of the tracer, high latitude north, equatorial region, high latitude south, and two sections of the current density at mid latitudes. In the left frame, pale blue isocontour surfaces of the magnitude of the current density show the mid-latitude current sheets, while blue and red lines represent pristine magnetospheric and interplanetary magnetic field lines crossing a northern current sheet. In the right frame, green and yellow lines represent once-reconnected magnetic field lines crossing a northern current sheet, while black and violet lines represent double-reconnected lines.

is provided at any fixed time t by the solution of the Eqs. (1)–(4). In order to make the computation of the field lines less time consuming while keeping the needed accuracy, we have adopted an approximate description of the perturbed magnetic field $\delta\mathbf{B} = \mathbf{B} - \mathbf{B_{eq}}$, where $\mathbf{B_{eq}} = \nabla \times A_{eq,y}\mathbf{e}_y$, following the procedure adopted in Ref. 30. In particular, only the modes obtained from the 3D Fourier decomposition of δB with amplitude larger then 10^{-5} have been considered, resulting in an accurate representation of the original data.

For illustration, in Fig. 7 we follow three field lines in the magnetic configuration at $t = 800$. In the upper frame, we give the trajectory components $x(z)$ and $y(z)$ of a doubly reconnected field line (MS → SW → MS, i.e., blue → red → blue) that reconnects close to mid latitude ($z = 90$ and $z = 270$ are marked by two dashed white lines). In the middle frame, we give the trajectory components of a doubly reconnected field line that reconnects somewhat closer to the equatorial region, while in the lower frame, we give the trajectory components of a singly reconnected field line (SW → MS, i.e., red → blue). Multiple crossings (such as triple or quadruple crossings) can also occur but most of them arise from trajectories passing through the tracer transition region.

C. 3D magnetic structures and mixing regions

In order to see how fast field lines that have reconnected once in one hemisphere get reconnected a second time in the

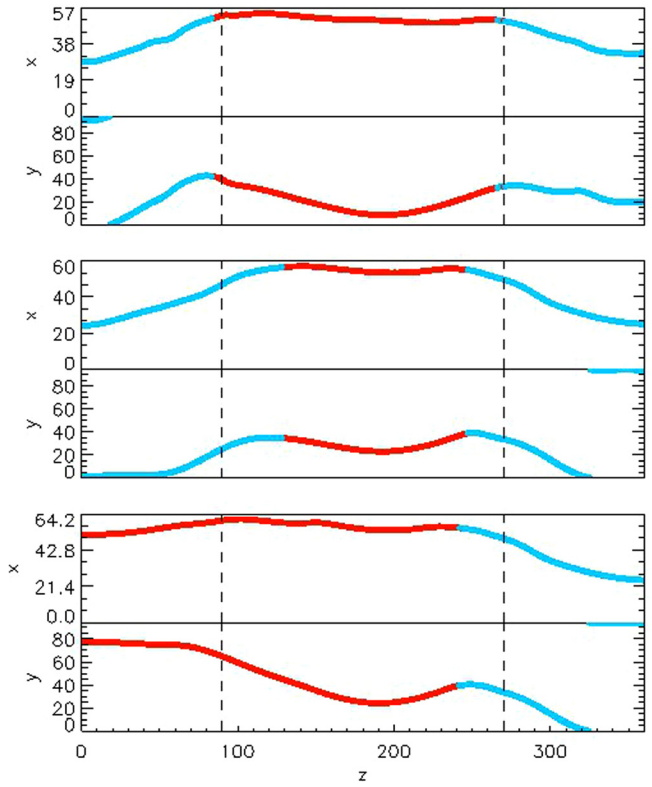

FIG. 7. Crossings of three field lines in the magnetic configuration at $t = 800$. The trajectory components $x(z)$ and $y(z)$ of two doubly reconnected field lines are shown in the upper and middle frames and that of a singly reconnected line in the bottom frame.

opposite hemisphere, we employ a method that resembles a Poincarè map: we plot the crossing points of a large set of field lines through an x-y section and mark the points with different colours depending on whether they correspond to field lines that have reconnected zero, one, or two times. This allows us to divide the selected ensemble of field lines into three "populations." An example of this method is shown in Fig. 8, where the spatial distribution of the once- (green) and double- (orange) reconnected magnetic field lines of the magnetic field at $t = 790$ is plotted at different latitudes. The magnetic field lines we considered rise from a set of initial conditions uniformly distributed on a slab domain at $z = -L_z/2$ enclosing all the reconnected regions.

We repeat this procedure at different times in the development of reconnection to see how these three populations evolved. We find, see Fig. 9, that the area of the doubly reconnected lines has indeed increased monotonically while the extent of the region crossed by singly reconnected lines remained almost constant between $t = 750$ and $t = 790$, or increased, but with a smaller rate compared to the double reconnected region, for $t < 750$ and $t > 790$. The fact that the population of singly reconnected lines remains always smaller than the population of the doubly reconnected lines implies that singly reconnected lines become doubly reconnected almost as soon as they are formed. This can be explained looking at the topology and dynamics of single reconnected lines. In fact once reconnection has occurred in one hemisphere (e.g., the northern one), the resulting lines, as shown by once-reconnected yellow and green lines in Fig. 6, right frame, become braided (they are connected to different plasmas at each of the two high latitude section). On the contrary, their feet are still advected in opposite directions by the unperturbed SW and MS velocity. This configuration strongly suggests that these lines must reconnect a second time in order to became unbraid and relax the magnetic tension.

The method employed, for obtaining the green and orange crossing points, differs from a true Poincarè map because in the Earth configuration, there is no physical periodicity in z and thus field lines are only followed along a single cycle from $-L_z/2$ to $L_z/2$. We start the field line integration close to the X-points located at the mid-latitude plane $z = -L_z/4$ and follow the field line up to $z = L_z/2$. After

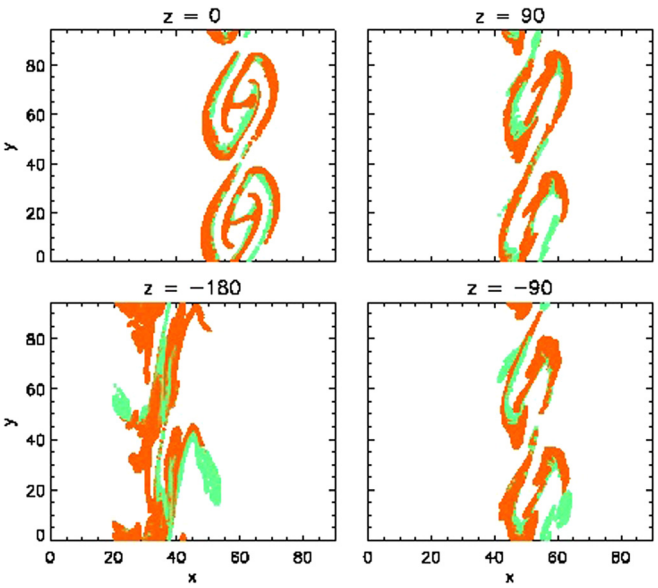

FIG. 8. Maps of the reconnected magnetic field line regions of the magnetic field at $t = 790$ on different latitudes. Orange regions are crossed by double-reconnected field lines, while once-reconnected field lines stay into the green regions. Magnetic field lines are computed starting from a uniform distribution of 512×512 initial conditions in the slab domain $20 < x < 55$, $-L_y < y < L_y$ at $z = -L_z/2$.

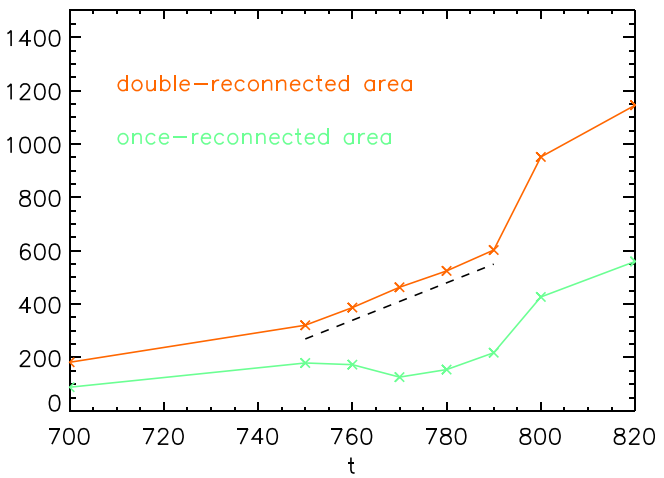

FIG. 9. Time evolution of the once- and double-reconnected area. The dashed line highlights the linear growth of the area of the double-reconnected magnetic field lines in the time interval $750 < t < 790$ where the normal component of the magnetic field grows as t^2.

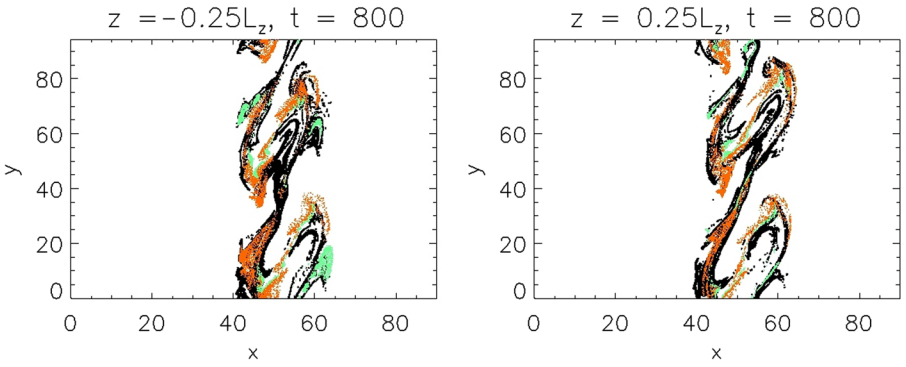

FIG. 10. Maps of the reconnected magnetic field line regions of the magnetic field at $t = 800$ on different latitudes. Orange regions are crossed by double-reconnected field lines, while once-reconnected field lines stay into the green regions. The black points represent the crossing of field lines whose initial conditions are taken close to the X-points located at $x = 50$, $y = 33.5$ $z = -90$ and $x = 52.2$, $y = 84$, $z = -90$.

one cycle is completed, we reinitialize the field line integration for a second cycle at the values of x and y reached by the field line but starting from $z = -L_z/2$. Due to the strong stretching of magnetic field lines, the crossing points (black points in Fig. 10) of these lines with the $z = +L_z/4$ plane and the $z = -L_z/4$ plane span the whole vortex structures and show that the magnetic structure is rolled-up by the vortices, with no clearly defined separatrix been identifiable. This Poincarè-like map allows us to visualize the cross-talking between the magnetic structure of the mid latitude current layers in the northern and in the southern hemispheres and the turning and twisting effects due to the KH vortices in the equatorial region. In fact, these maps display rather complex and filamented structures where ropes of field lines that have undergone no reconnection and ropes of field lines that have reconnected once or twice are intertwined and not show the usual topological properties that characterize 2D systems.

The number of crossings of doubly reconnected field lines increases approximately linearly in time, as shown in Fig. 9, in the time interval $750 < t < 790$. This is consistent with an increase proportional to the area of the reconnection region, as estimated from the t^2 growth of the perturbed perpendicular field in the Rutherford saturated regime.

In Ref. 20, it was shown that a growth of the double-reconnected area, linear in time and with a rate of the order of the Alfvén velocity times the ion skin depth, can account for the observed influx of SW particles into the MS. Here, we make this estimate more quantitative by referring to the Poincarè-like maps shown in Fig. 8. This allows us to determine the double-reconnected area A_λ per KH wavelength and its time derivative $dA_\lambda/dt \simeq 3\ V_A d_i$. The amount of SW matter that enters the MS via the double reconnection process is given, looking at double-reconnected flux tubes that are connected to the Earth in both hemispheres, by the SW plasma density times the overall volume of all the portions of these tubes that are embedded in the SW, i.e., by $Q_\lambda \simeq 1/2\ \rho_{SW}\ A_\lambda\ L_z/2$, where $L_z/2$ represents the averaged distance between the reconnection sites and the factor 1/2 takes into account the fact that only one-half of the double-reconnected tubes is connected to the Earth. Comparing the mass flux through the magnetospheric border $J_\lambda = dQ_\lambda/dt/(\lambda L_z)$ with that given by a simplified diffusion model that takes into account the width L_{eq} of the magnetopause and the gradient of the plasma density, $D_{eff}\nabla\rho \sim \rho_{SW}/L_{eq}$, we infer the value of the effective diffusion coefficient associated with the double mid-latitude reconnection process: $D_{eff} \simeq 1/4\ L_{eq}/\lambda\ dA_\lambda/dt \simeq 1/20\ V_A d_i$. Taking $V_A \simeq 300$ km/s and $d_i \simeq 250$ km as representative of the typical plasma quantities at the outer MS, we find $D_{eff} \sim O(10^9)$ m^2/s. This order of magnitude is the same as that of the diffusion coefficient that is required for explaining the observed transport adopting a simplified viscous model of the magnetopause.[31]

IV. CONCLUSIONS

Magnetic field line reconnection plays a fundamental role in the mixing of different regions of a magnetized plasma that would otherwise remain separate because of topological constraints. In the present paper, we clarify a number of important features of this process by investigating in a 3D geometry the inflow of the solar wind plasma into the Earth's magnetosphere caused by magnetic reconnection induced by the Kelvin-Helmholtz instability at the flanks of the magnetosphere. In this configuration, reconnection is neither prepared by the initial magnetic field conditions nor is imposed by special boundary conditions. We find that despite the fully 3D approach we employ, in the Earth's magnetospheric configuration *locally*, the reconnection process develops initially in a quasi-2D fashion, rather similarly to standard models where a guide field is present and a magnetic inversion of the magnetic shear component is imposed at t = 0. We provide evidence of the instability exponential growth in its linear phase followed by a parabolic growth in time in its nonlinear phase.

Most important, we show that at a *global scale*, the 3D dynamics is essential in explaining how field lines that reconnect once in one hemisphere are forced to reconnect again in the opposite hemisphere. This "mid-latitude double reconnection process," investigated in Ref. 20, has been confirmed here by following a large set of individual field lines using a method similar to a Poincarè map.

The mid-latitude reconnection process is driven by the formation of nearly 2D KH vortices at low latitude. These vortices stretch and advect the magnetospheric field lines following the vortices 2D geometry. In a magnetized weakly collisional or collisionless plasma, such action at a distance can convey stresses and energy through the propagation of Alfvèn waves far from the region where these stresses are exerted: for example, it is present in the dynamics of magnetic structures in closed regions of solar and stellar coronae threaded by magnetic field lines that are line-tied at two dense plasma regions moving with different velocities that are modeled in Ref. 32 as oscillating conducting plates. A sort of complementary configuration is found at the flanks of

the Earth's MS in the transition between the MS plasma and the SW plasma when the interplanetary magnetic field is northward. In this case, the role of the oscillating plates is played by the rotation and advection of the KH vortices in the equatorial regions that twist field lines that are line-tied either to the Earth's poles or to the streaming SW plasma. The resulting action at a distance leads to the formation of current layers, and eventually to magnetic field line reconnection, at mid latitudes, i.e., far from the region where the KH vortices are formed. Field lines are initially tied on both sides either to the streaming SW or to the Earth poles. Reconnection creates field lines that are tied on one side to Earth and on the other to the SW. The stretching due to the different advection velocity of the two reconnected field line sides make them reconnect a second time, this time in the opposite hemisphere, so as to restore the initial tying. In this process magnetic field lines are created that are tied to Earth on both sides but enter the SW in a region on the two sides of the equatorial plane. Such field lines provide an efficient channel for penetration of the SW plasma into the MS as discussed in Refs. 20 and 25. In the present article, a more quantitative evaluation of the amount of plasma involved in this process is presented by tracing the time evolution of the area corresponding to double reconnected field lines explicitly by means of Poincarè-like map which confirms the previous estimate and is consistent with the observed plasma transport. Finally, we have shown how the intrinsic 3D nature of the double magnetic field lines reconnection leads to the generation of twisted magnetic structures that exhibit spatial features that differ from quasi-2D magnetic islands.

ACKNOWLEDGMENTS

The research leading to these results has received funding from the European Commission's Seventh Framework Programme (FP7/2007-2013) under the Grant Agreement SWIFF (Project No. 263340, www.swiff.eu). We acknowledge the access to supermuc machine at LRZ made available within the PRACE initiative receiving funding from the European Commission's Seventh Framework Programme (FP7/2007-2013) under Grant Agreement No. RI-283493, Project No. 2012071282.

[1]J. W. Dungey, "Electrodynamics of the outer atmosphere," in *Proceedings of the Conference of the Ionosphere* (Physical Society of London, London, 1955), p. 255.
[2]T. D. Phan, L. M. Kistler, B. Klecker, G. Haerendel, G. Paschmann, B. U. Ö. Sonnerup, W. Baumjohann, M. B. Bavassano-Cattaneo, C. W. Carlson, A. M. DiLellis, K.-H. Fornacon, L. A. Frank, M. Fujimoto, E. Georgescu, S. Kokubun, E. Moebius, T. Mukai, M. Øieroset, W. R. Paterson, and H. Reme, Nature **404**, 848 (2000).
[3]N. G. Sckopke, G. Paschmann, G. Haerendel, B. U. O. Sonnerup, S. J. Bame, T. G. Forbes, E. W. Hones, Jr., and C. T. Russell, J. Geophys. Res. **86**, 2099, doi:10.1029/JA086iA04p02099 (1981).
[4]K. Nykyri and A. Otto, Geophys. Res. Lett. **28**, 3565, doi:10.1029/2001GL013239 (2001).
[5]T. K. M. Nakamura, H. Hasegawa, I. Shinohara, and M. Fujimoto, J. Geophys. Res. **116**, A03227, doi:10.1029/2010JA016046 (2011).
[6]T. K. M. Nakamura, M. Fujimoto, and A. Otto, J. Geophys. Res. **113**, A09204, doi:10.1029/2007JA012803 (2008).
[7]P. Henri, S. S. Cerri, F. Califano, F. Pegoraro, C. Rossi, M. Faganello, O. Šebek, P. M. Trávníek, P. Hellinger, J. T. Frederiksen, A. Nordlund, S. Markidis, R. Keppens, and G. Lapenta, Phys. Plasmas **20**, 102118 (2013).
[8]A. Miura, Phys. Plasmas **4**, 2871 (1997).
[9]P. Henri, F. Califano, M. Faganello, and F. Pegoraro, Phys. Plasmas **19**, 072908 (2012).
[10]M. Faganello, F. Califano, and F. Pegoraro, Phys. Rev. Lett. **100**, 015001 (2008).
[11]M. Faganello, F. Califano, and F. Pegoraro, Phys. Rev. Lett. **101**, 105001 (2008).
[12]M. Faganello, F. Califano, and F. Pegoraro, Phys. Rev. Lett. **101**, 175003 (2008).
[13]A. Otto and D. H. Fairfield, J. Geophys. Res. **105**, 21175, doi:10.1029/1999JA000312 (2000).
[14]A. Tenerani, M. Faganello, F. Califano, and F. Pegoraro, Plasma Phys. Controlled Fusion **53**, 015003 (2011).
[15]M. Faganello, F. Califano, and F. Pegoraro, New J. Phys. **11**, 063008 (2009).
[16]S. Eriksson, H. Hasegawa, W.-L. Teh, B. U. Ö. Sonnerup, J. P. McFadden, K.-H. Glassmeier, O. Le Contel, V. Angelopoulos, C. M. Cully, D. E. Larson, R. E. Ergun, A. Roux, and C. W. Carlson, J. Geophys. Res. **114**, A00C17, doi:10.1029/2008JA013505 (2009).
[17]T. K. M. Nakamura, W. Daughton, H. Karimabadi, and S. Eriksson, J. Geophys. Res. Space Phys. **118**, 5742, doi:10.1002/jgra.50547 (2013).
[18]W. Daughton, V. Roytershteyn, H. Karimabadi, L. Yin, B. J. Albright, B. Bergen, and K. J. Bowers, Nat. Phys. **7**, 539 (2011).
[19]D. Borgogno, D. Grasso, F. Califano, D. Farina, F. Pegoraro, and F. Porcelli, Phys. Plasmas **12**, 032309 (2005).
[20]M. Faganello, F. Califano, F. Pegoraro, and T. Andreussi, Europhys. Lett. **100**, 69001 (2012).
[21]M. Faganello, F. Califano, F. Pegoraro, T. Andreussi, and S. Benkadda, Plasma Phys. Controlled Fusion **54**, 124037 (2012).
[22]S. V. Bulanov, J. Sakai, and S. I. Syrovatskii, Sov. J. Plasma Phys. **5**, 157 (1979).
[23]D. Biskamp, Phys. Fluids **29**, 1520 (1986).
[24]Y.-M. Huang and A. Bhattacharjee, Phys. Plasmas **20**, 055702 (2013).
[25]M. Faganello, F. Califano, F. Pegoraro, and A. Retinò, Europhys. Lett. **107**, 19001 (2014).
[26]S. K. Lele, J. Comput. Phys. **103**, 16 (1992).
[27]T. Andreussi, P. J. Morrison, and F. Pegoraro, Phys. Plasmas **19**, 052102 (2012).
[28]P. H. Rutherford, Phys. Fluids **16**, 1903 (1973).
[29]Y. Matsumoto and M. Hoshino, Geophys. Res. Lett. **31**, L02807, doi:10.1029/2003GL018195 (2004).
[30]D. Borgogno, D. Grasso, F. Pegoraro, and T. J. Schep, Phys. Plasmas **15**, 102308 (2008).
[31]B. U. Ö. Sonnerup, J. Geophys. Res. **85**, 2017, doi:10.1029/JA085iA05p02017 (1980).
[32]A. F. Rappazzo and E. N. Parker, Astrophys. J. **773**, L2 (2013).